



In-vitro* investigation of biofilm-specific resistance and virulence of biofilm-forming uropathogenic *Escherichia coli

Sara A. Alshaikh^{*}; Tarek El-Banna; Fatma Sonbol; Mahmoud H. Farghali

Department of Microbiology and Immunology, Faculty of Pharmacy, Tanta University, Tanta, Gharbia, Egypt

^{*}Corresponding author E-mail: sara.alshaikh@pharm.tanta.edu.eg



Received: 14 December, 2023; Accepted: 14 January, 2024; Published online: 17 January, 2024

Abstract



Copyright policy

NRMJ allows the author(s) to hold the copyright, and to retain publishing rights without any restrictions. This work is licensed under the terms and conditions of the Creative Commons Attribution (CC BY) license (<https://creativecommons.org/licenses/by/4.0/>)

Uropathogenic *Escherichia coli* (UPEC) is the primary etiologic agent of urinary tract infections (UTIs). This study aimed to investigate the difference in antimicrobial susceptibility of UPEC isolates in the planktonic and biofilm states. Important virulence factors were also evaluated. The minimum inhibitory concentrations (MICs) were determined and recorded as 0.5-64 µg/ml for amikacin, 0.5-64 µg/ml for cefotaxime, 0.25-64 µg/ml for cefepime, 0.25-16 µg/ml for meropenem, and 0.125-32 µg/ml for ciprofloxacin. Biofilm-specific resistance was assessed using the minimum biofilm eradication concentration (MBEC). The obtained results for MBEC were: 8-512 µg/ml for amikacin, 32-512 µg/ml for cefotaxime, 8-512 µg/ml for cefepime, 4-256 µg/ml for meropenem, and 4-128 µg/ml for ciprofloxacin. The virulence factors were evaluated using suitable phenotypic techniques. Our findings revealed a significant enhancement in the antimicrobial resistance after biofilm formation. The MBEC values were higher than the MIC values by 2-128 folds for amikacin, 2-256 folds for cefotaxime, 2-64 folds for cefepime, 8-128 folds for meropenem, and 4-128 folds for ciprofloxacin. The swimming and swarming motilities demonstrated a significant positive correlation ($r_s = 0.506$, $P < 0.001$). Protease production analysis revealed a large variation, with the weak biofilm-producing isolates EW2 and EW15 displaying the largest zone diameters of 39 mm and 33 mm; respectively. We have also evaluated the distribution and levels of siderophore production, which were significantly associated with meropenem resistance. Finally, this study underscores the importance of considering biofilm formation in UPEC treatment and emphasizes the need for therapeutics targeting these biofilms.

Keywords: Uropathogenic *Escherichia coli*, Biofilm, Minimum inhibitory concentration, Minimum biofilm eradication concentration, Virulence factors

1. Introduction

Urinary tract infections (UTIs) are among the most prevalent human infections caused by bacteria. In 2019, UTIs resulted in 230,000 deaths globally ([Terlizzi *et al.*, 2017](#); [Whelan *et al.*, 2023](#)). Uropathogenic *Escherichia coli* (UPEC) is the primary etiology of UTIs, accounting for up to 95 % of the community-acquired UTIs and 40 % of the healthcare-associated UTIs ([Gajdács *et al.*, 2021b](#); [Walker *et al.*, 2022](#)).

According to [Sundaramoorthy *et al.*, \(2022\)](#), UPEC strains can form biofilms that shield the embedded bacterial cells from the environmental stressors, antimicrobial agents, and the host's immune system. Therefore, biofilm formation is closely linked to the bacterial resistance and is known to encourage the persistence and recurrence of these bacterial infections. [Ballén *et al.*, \(2022a\)](#); [Thöming and Häussler, \(2022\)](#) added that the bacteria in biofilms display dramatic improvement in the antimicrobial resistance due to various factors, including reduced antimicrobial diffusion, slowed multiplication, upregulation of resistance determinants, and the development of persister cells. The persister cells are small percentage of a biofilm population that becomes dormant due to its minimal metabolic activity. Since the antibiotics mainly attack the actively growing cells, the persister cells can survive in high antibiotic doses and resume their normal growth after treatment cessation ([Bottery *et al.*, 2021](#)). The association between biofilm formation and resistance has been the subject of extensive researches. [Ballén *et al.*, \(2022b\)](#) observed that biofilm formation in *E. coli* increases the antimicrobial resistance. On the other hand, several studies showed that antibiotic resistance may have a fitness cost on the bacterial cells, which could negatively affect the biofilm formation ([Shenkutie *et al.*, 2020](#); [Yamani *et al.*, 2021](#)). Meanwhile, [Carcione *et al.*, \(2022\)](#); [Donadu *et al.*, \(2022\)](#) studies reported no link between the development of biofilms and antibiotic resistance. The microbiological laboratories

recommend an antimicrobial therapy based on the resistance of the planktonic cells, which is determined using standard antimicrobial susceptibility assays, such as determination of the minimum inhibitory concentration (MIC). However, these assays do not evaluate susceptibility of the bacteria in biofilms ([Shenkutie *et al.*, 2020](#)). The difference in antimicrobial susceptibility between the planktonic and the biofilm-associated cells may explain the frequent therapy failure and recurrence in the cases of biofilm-forming infections ([Bottery *et al.*, 2021](#)). The biofilm-related antimicrobial susceptibility can be measured using the minimum biofilm eradication concentration (MBEC), which is the lowest antibiotic concentration needed to inhibit regrowth of the pre-formed biofilms ([Ciofu *et al.*, 2022](#)).

Additionally, different virulence factors possessed by UPEC enable it to colonize, invade the host tissues, and to survive against the host defense mechanisms ([Ambite *et al.*, 2021](#); [Torres-Puig *et al.*, 2022](#)). These virulence factors include flagellar motility, protease and siderophore production. Flagellar motility that facilitates UPEC ascension in the urinary tract includes the swimming and swarming motilities. The swarming motility describes the multicellular movement of the bacteria across a surface, while the swimming motility refers to the movement of the individual cells in the liquid media ([Vega-Hernández *et al.*, 2021](#); [Wadhwa and Berg, 2022](#)). The proteases have an important role in facilitating the host tissue invasion, and they also significantly contribute to the immune evasion capacity of UPEC ([Freire *et al.*, 2022](#); [Chen *et al.*, 2023](#)). A previous study reported by [Subashchandrabose and Mobley, \(2015\)](#) that the ability of UPEC to competitively chelate iron from the host tissues using siderophores ensures its survival in the iron-scarce environment of the urinary tract. The objective of this study was to evaluate how the planktonic and the biofilm-embedded UPEC isolates, which have different biofilm formation capacities,

vary in their antimicrobial susceptibilities. Furthermore, several virulence factors of UPEC were evaluated, including motility, protease and siderophore production.

2. Materials and methods

2.1. Sampling of the *Escherichia coli* isolates

Clinical UPEC isolates (n = 46) with different biofilm-forming abilities, namely, strong (n = 15), moderate (n = 15), and weak (n = 16) that were previously determined (unpublished data), were obtained from Tanta University Hospital, Tanta, Gharbia governorate, Egypt.

2.2. Determination of the minimum inhibitory concentration (MIC)

The minimum inhibitory concentrations (MICs) were determined for the forty six UPEC isolates using the standard broth microdilution method ([CLSI, 2020](#)), for the following antibiotics: ciprofloxacin (CIP), amikacin (AK), cefotaxime (CTX), cefepime (CPM), and meropenem (MRP). The MIC determination assay was repeated twice with three replicates for each treatment, to ensure reproducibility and accuracy of the recorded MICs.

2.3. Determination of the minimum biofilm eradication concentration (MBEC)

To study the difference in antibiotic susceptibility between the planktonic and the biofilm-embedded cells of the forty six UPEC isolates, the biofilm-specific resistance was determined by measuring the minimum biofilm eradication concentration (MBEC) for the five tested antibiotics. Initially, the isolates were allowed to form biofilms in 96-well microtiter plates, as previously described by [Ballén *et al.*, \(2022b\)](#). Following the biofilm formation, the MBEC assay was carried out as detailed by [Rafaque *et al.*, \(2020\)](#). The broth medium (minimal M63) was carefully removed from the wells, and a sterile phosphate-buffered saline (PBS) was used to wash the wells three times. Antibiotics ranging in concentration

from 0.5 to 2048 µg/ml were then prepared in two-fold serial dilutions, and 100 µl of each concentration was applied aseptically and individually to the wells. The plates were then incubated at 37 °C for 24 h. After incubation, the antibiotic solutions were removed and the wells were washed with PBS, and then 100 µl of Luria Bertani (LB) broth was added to each well, and then the wells were examined for bacterial growth. Wells that showed no signs of growth or turbidity were carefully scraped using a sterile micro-pipette tip, with special attention paid to the well's edges. The scraped material was transferred into 1 ml of PBS. After brief vortexing to break up the biofilms, 100 µl of each sample suspension was plated onto a sterile tryptic soy agar (TSA) plate, followed by incubation for 24 h at 37 °C. After incubation, the lowest concentration that showed no visible colonies on TSA plates was considered as the MBEC. The MBEC assay was performed twice with three replicates for each treatment, to ensure reproducibility and accuracy of the MBEC.

2.4. Growth curve analysis

As previously described by [Hung *et al.*, \(2012\)](#), the growth rates of the forty six UPEC isolates of various biofilm formation categories were examined. After growing the UPEC isolates on nutrient agar (NA) for 24 h at 37 °C, the growing cells were suspended in a sterile 0.9 % saline solution and adjusted to 0.5 McFarland units. Afterward, these bacterial suspensions were diluted in LB broth by a factor of 1:20, and the mixture was incubated for 24 h at 37 °C with agitation at 200 rpm. The optical density at 600 nm (OD₆₀₀) values were measured using a UV-Vis spectrophotometer (Shimadzu™, Japan) after the following periods: 0 h, 2 h, 4 h, 6 h, 8 h, 10 h, 12 h, and at 24 h. The measured OD₆₀₀ values were used to create the growth curve for each tested isolate.

2.5. Swimming and swarming motility assays

Determination of the swimming and swarming motilities was performed according to [Pearson, \(2019\)](#) with minor modifications. Briefly, LB broth medium

with agar concentrations of 0.3 % for the investigation of the swimming motility and 1 % for investigation of the swarming motility were used. For evaluation of the swimming motility, overnight bacterial cultures of each UPEC isolate were adjusted to a density of $OD_{600} = 1.0$. Subsequently, the cultures were inoculated individually and inserted vertically into the motility agar medium using a sterile inoculating needle. Care was taken during inoculation to avoid pushing the needle through the bottom of the Petri plate, and to ensure that the needle remains vertical during insertion and withdrawal. For evaluating the swarming motility, the swarm agar plates were surface inoculated individually with 5 μ l of the overnight bacterial culture, which was adjusted to $OD_{600} = 1.0$. After incubation of all plates at 37 °C for 24 h, the growth zone diameters were measured in mm using a calibrated ruler. The swarming and swimming motility assays were performed in triplicates, and the average zone diameter was calculated and approximated to the nearest mm.

2.6. Protease production

Uropathogenic *E. coli* isolates (n = 64) were tested qualitatively for their ability to produce proteases according to the previously established method of [Alnahdi, \(2012\)](#). Briefly, the isolates were inoculated individually onto skim milk agar plates containing 5 % skimmed milk in 1.5 % LB agar. After incubation for 48 h at 28 °C, the positive protease production was depicted as a clear zone surrounding the bacterial growth due to proteolysis. This assay was conducted twice with three replicates for each treatment. Moreover, protease production levels were determined semi-quantitatively according to [Seleem *et al.*, \(2021\)](#). Overnight cultures of UPEC isolates in LB broth were centrifuged at 10,000 rpm for 20 min. at 4 °C, and then a 0.22 μ m filter was used to remove the bacterial cells and obtain a sterile supernatant. Wells in the skim milk agar medium were made using a sterile cork borer (three wells for each isolate), and 100 μ l of the sterile protease-containing supernatants was added individually to these wells. After 24 h of incubation at 37 °C, protease diffusing from the wells led to

proteolysis of the casein present in the agar media, causing the formation of clear zones around the wells. The zone diameters were measured in mm. A well containing LB broth instead of the bacterial supernatant was used as a negative control.

2.7. Siderophore production estimation

Quantitative determination of siderophore production was carried out for all the tested isolates (n= 46), as previously described by [Eger *et al.*, \(2022\)](#). Briefly, 0.5 McFarland suspension of the bacterial isolates was prepared individually in sterile saline, and 50 μ l from each suspension was added aseptically to 15 ml of M9 minimal broth medium, which was supplemented with 0.3 % casamino acids, 2 mM $MgSO_4$, and 200 μ M 2,2'-dipyridyl. The cultures were incubated at 37 °C, at 130 rpm for 24 h. After incubation, the bacterial cultures were centrifuged at 7000 rpm for 20 min., and 100 μ l of the supernatant was added to a 96-well microtiter plate. In each well, 100 μ l of the Chrome Azurol S-Hexadecyltrimethylammonium bromide (CAS-HDTMA) solution prepared according to [Neilands, \(1987\)](#) was added to the culture supernatant. A blank medium supplemented with the CAS reagent was used as a negative control, while a 15 mM Ethylene diamine tetra acetic acid (EDTA) solution with the CAS reagent was used as a positive control. Subsequently, the mixtures were incubated for 30 min. at ambient temperature in darkness, and then the absorbance was measured at 630 nm using a microplate reader (Sunrise™, TECAN, Switzerland). The assay was carried out in triplicates and the average absorbance was considered. The siderophore production level was calculated using the Percent Siderophore Unit (PSU), according to [Arora and Verma, \(2017\)](#):

$$PSU = \frac{(Ar-As)}{Ar} \times 100$$

Where; Ar = reference absorbance (CAS-HDTMA solution in sterile broth) and As = sample absorbance (CAS-HDTMA solution in cell-free sample supernatant).

2.8. Statistical analysis

The Statistical Package for the Social Sciences (SPSS) software, version 27.0 (IBM Corp., Armonk, NY, USA) was used to conduct statistical analyses. All P-values were two-tailed and were regarded as statistically significant at the $P < 0.05$ level. The chi-square test was used to evaluate the connections between the categorical variables. For intergroup comparisons and to investigate the correlation between numerical variables, a Spearman's rank correlation was applied. The Kruskal-Wallis test or the Mann-Whitney U test was employed to compare the numerical variables amongst the different groups. The Kruskal-Wallis test was followed by pairwise comparisons and a Bonferroni adjustment for multiple comparisons.

3. Results

3.1. MIC and MBEC determination

The MICs and the MBECs of amikacin, cefotaxime, cefepime, meropenem, and ciprofloxacin for 46 UPEC isolates of different biofilm formation categories were determined and compared, in order to assess whether the biofilm-specific resistance is dependent on the biofilm quantity and/or on the antibiotic resistance in the planktonic mode. For cefotaxime, the resulting MIC values varied from 0.5 to 64 $\mu\text{g}/\text{ml}$. Cefotaxime MBECs ranged from 32 to 512 $\mu\text{g}/\text{ml}$. The MICs and MBECs for meropenem were 0.25–16 $\mu\text{g}/\text{ml}$ and 4–256 $\mu\text{g}/\text{ml}$; respectively. The MICs for ciprofloxacin ranged from 0.125 to 32 $\mu\text{g}/\text{ml}$, while the MBECs had a range of 8–512 $\mu\text{g}/\text{ml}$. Amikacin had MICs ranging from 0.5 to 64 $\mu\text{g}/\text{ml}$ and MBECs ranging from 8 to 512 $\mu\text{g}/\text{ml}$. The MICs and MBECs for cefepime varied from 0.25 to 64 $\mu\text{g}/\text{ml}$ and 8 to 512 $\mu\text{g}/\text{ml}$, respectively (Fig. 1-3).

The extent of resistance enhancement upon biofilm formation was measured by the fold differences between the MBEC and MIC values for each isolate, which was calculated by dividing the MBEC by the MIC values. For cefotaxime, MBEC values were 2–256 times higher than their corresponding MIC values. For meropenem, there was a 8–128 fold increase in the

MBECs over the corresponding MIC values. For ciprofloxacin, the MBECs were 4–128 times greater than the corresponding MIC values. For amikacin, the MBEC values were 2–128 folds greater than their corresponding MIC values. For cefepime, the MBEC values are 2–64 times higher than their corresponding MICs. The correlation between MIC values of the 46 isolates and their biofilm formation category was analyzed. Using Spearman's correlation analysis, a significant negative correlation between the two qualities for all of the tested antibiotics was detected; namely, AK ($r_s = -0.486$, $P < 0.001$), MRP ($r_s = -0.676$, $P < 0.001$), CTX ($r_s = -0.635$, $P < 0.001$), CPM ($r_s = -0.519$, $P < 0.001$), and CIP ($r_s = -0.407$, $P < 0.01$). These results were confirmed using the Kruskal Wallis analysis, which demonstrated the significant difference in MIC values among the different biofilm formation categories for all the tested antibiotics ($P < 0.05$) (Fig. 4).

By assessing the relationship between MIC and MBEC values, a positive correlation for all the tested antibiotics ($r_s = 0.861-0.473$, $P < 0.001$) was detected. The recorded difference between MIC and MBEC values demonstrated that biofilm formation indeed promotes the resistance of the bacterial isolate compared with the planktonic state. However, for most of the tested isolates, the level of resistance improvement following biofilm formation was almost the same. According to Spearman's rank correlation analysis, there was no significant correlation between the biofilm-related resistance (MBEC) and the biofilm density of the isolates ($r_s = -0.228-0.113$, $P > 0.05$). This indicates that different levels of biofilm density (i.e., strong, weak, and moderate) provided similar enhancement level in the antibiotic resistance.

3.2. Growth curve analysis

The growth rates of the strong, moderate, and weak UPEC biofilm formers did not differ significantly (Fig. 5), suggesting that the growth rate was not the cause of the variation in the biofilm formation levels and/ or the biofilm-specific resistance.

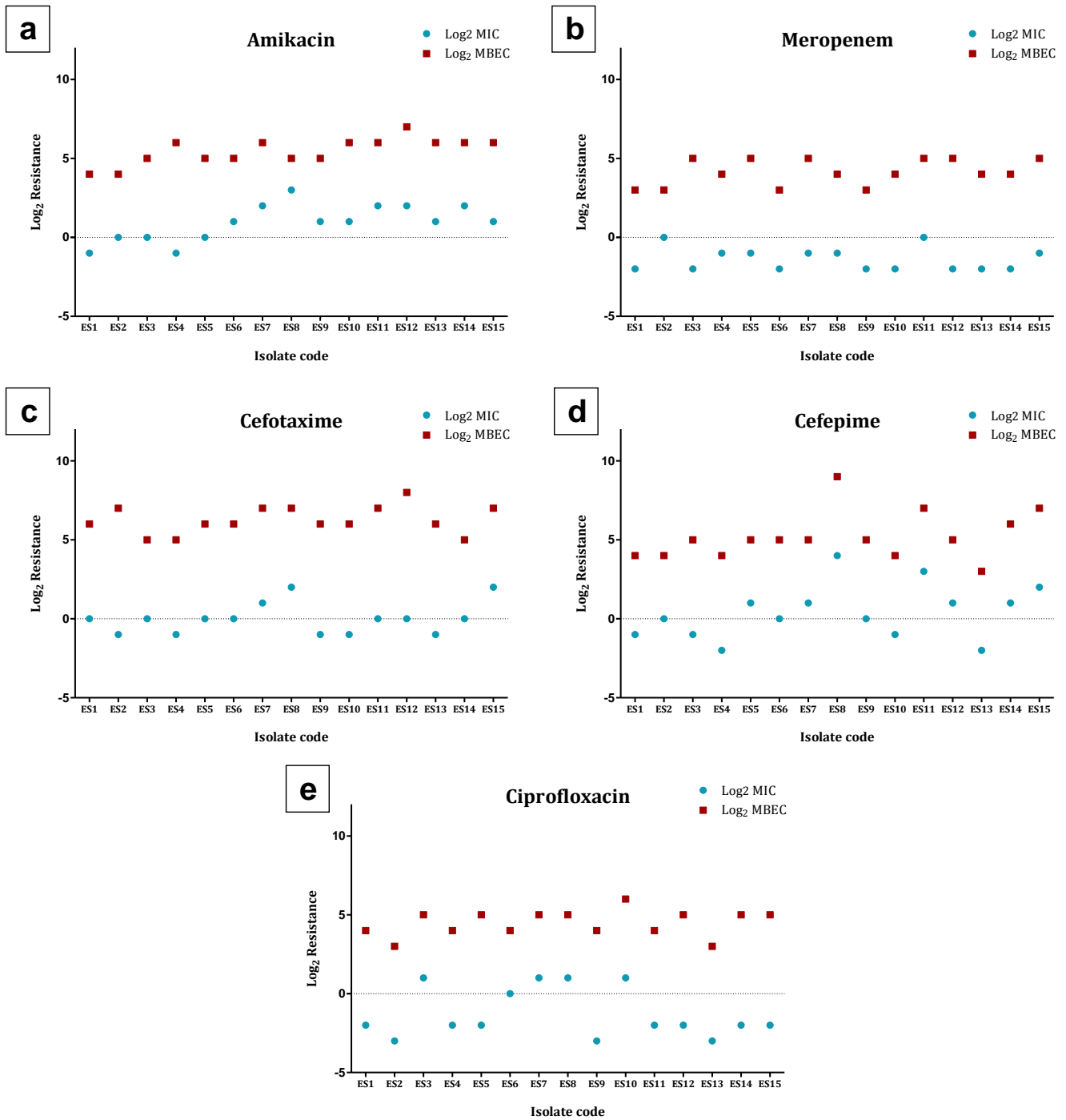


Fig. 1: Determination of the MBEC and MIC values of the 15 strong biofilm-forming UPEC isolates for amikacin (a), meropenem (b), cefotaxime (c), cefepime (d), and ciprofloxacin (e). The X-axis represents the isolate code, while the Y-axis represents log₂ of resistance (MIC or MBEC) for each isolate. The blue dots indicate the log₂ MIC, while the red squares indicate the log₂ MBEC. MIC: minimum inhibitory concentration. MBEC: minimum biofilm eradication concentration.

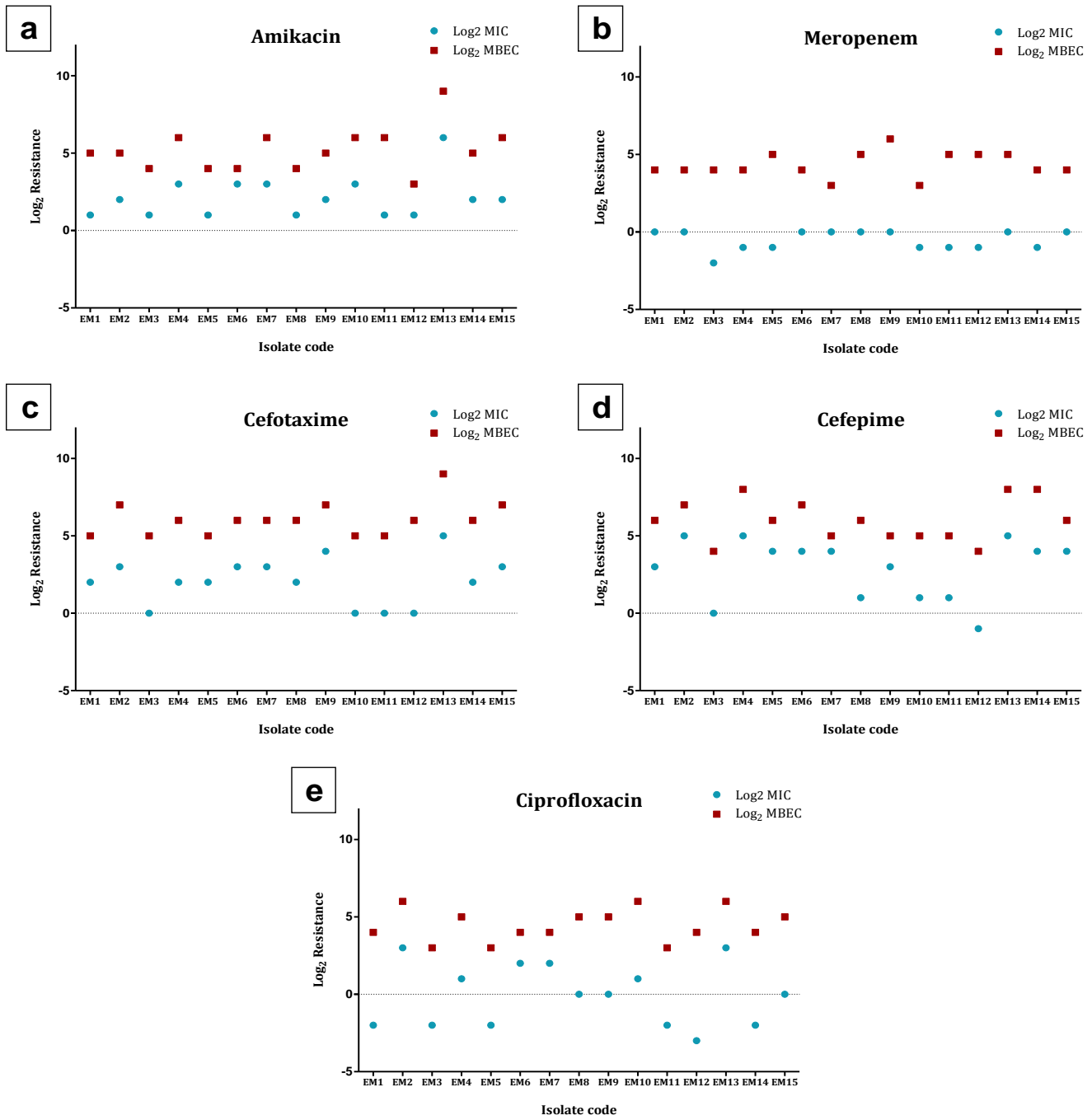


Fig. 2: Determination of the MBEC and MIC values of 15 moderate biofilm-forming UPEC isolates for amikacin (a), meropenem (b), cefotaxime (c), cefepime (d), and ciprofloxacin (e). The X-axis represents the isolate code, while the Y-axis represents log₂ of resistance (MIC or MBEC) for each isolate. The blue dots indicate the log₂ MIC, while the red squares indicate the log₂ MBEC. MIC: minimum inhibitory concentration. MBEC: minimum biofilm eradication concentration.

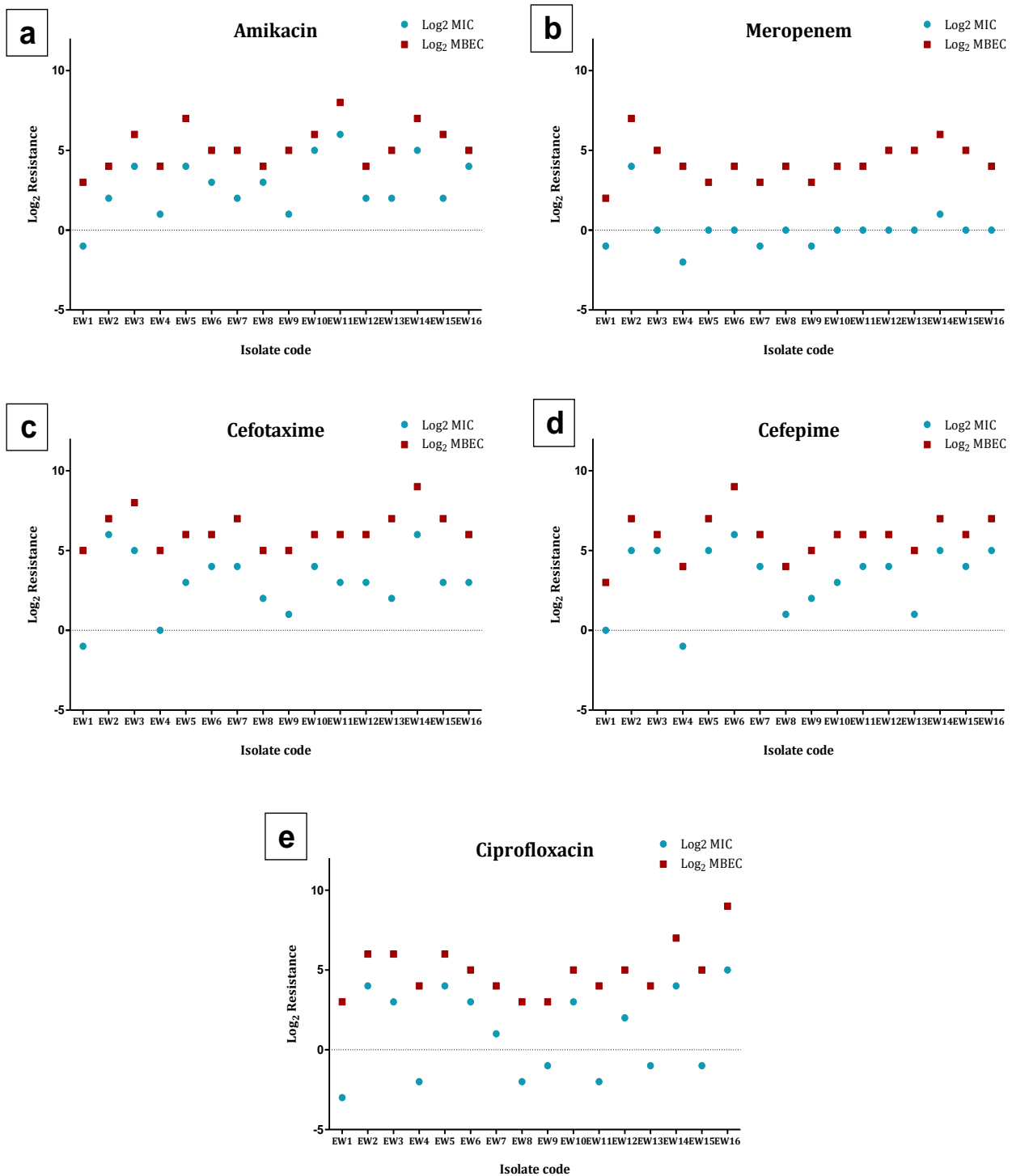


Fig. 3: Determination of the MBEC and MIC values of 16 weak biofilm-forming UPEC isolates for amikacin (a), meropenem (b), cefotaxime (c), cefepime (d), and ciprofloxacin (e). The X-axis represents the isolate code, while the Y-axis represents log₂ of resistance (MIC or MBEC) for each isolate. The blue dots indicate the log₂ MIC, while the red squares indicate the log₂ MBEC. MIC: minimum inhibitory concentration. MBEC: minimum biofilm eradication concentration.

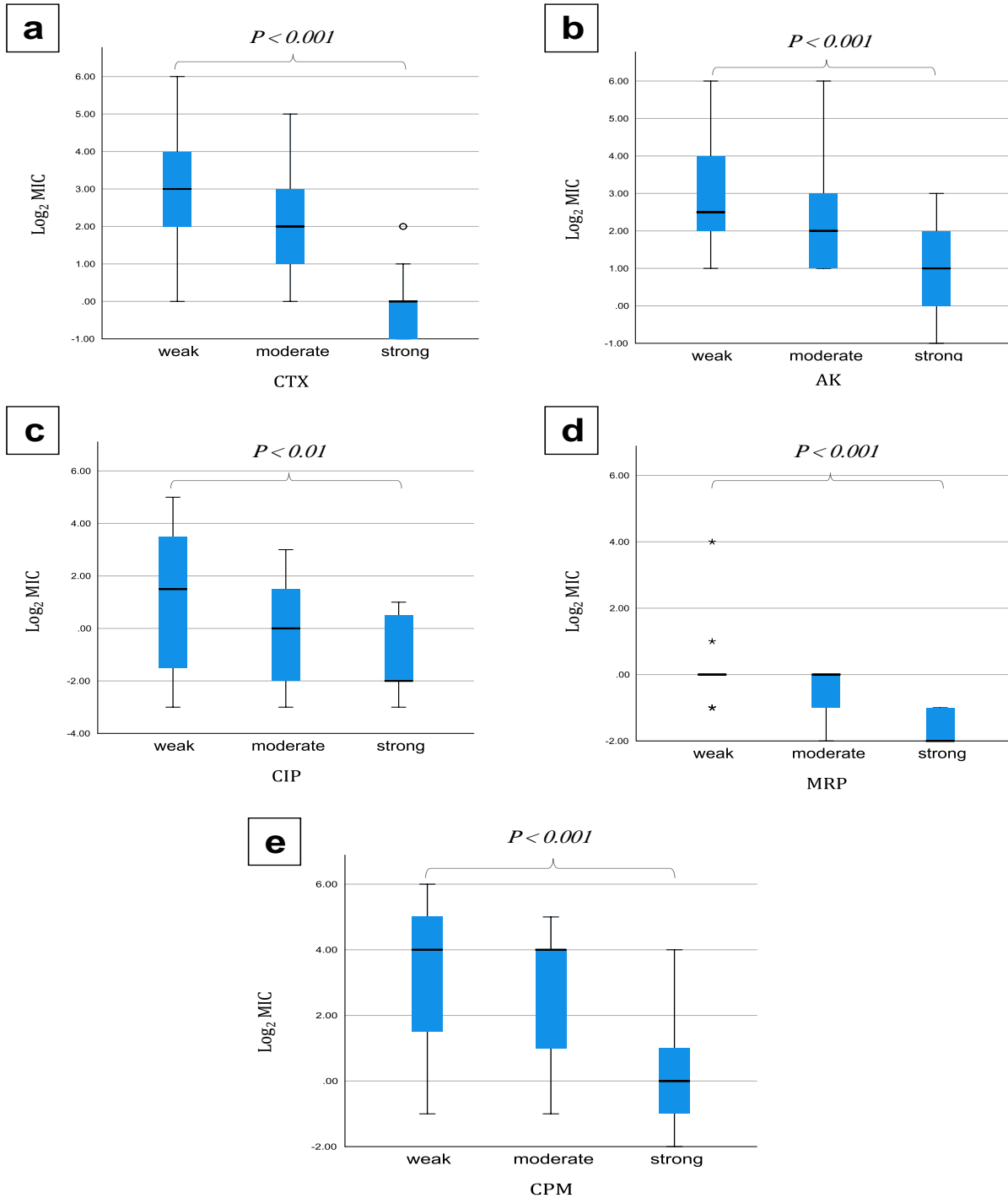


Fig. 4: Differences in MIC values of the tested UPEC isolates (n = 46) among the different biofilm formation categories including strong biofilm-producers (n = 15), moderate biofilm-producers (n = 15), and weak biofilm-producers (n = 16). The panels represent the distribution of the MIC values for cefotaxime (a), amikacin (b), ciprofloxacin (c), meropenem (d), and cefepime (e). The X-axis represents the biofilm formation category, while the Y-axis represents the log₂ of the MIC. The black dots represent the outlier values. MIC: minimum inhibitory concentration. This figure demonstrates the inverse correlation between the planktonic resistance levels and the biofilm formation category for all the tested antibiotics.

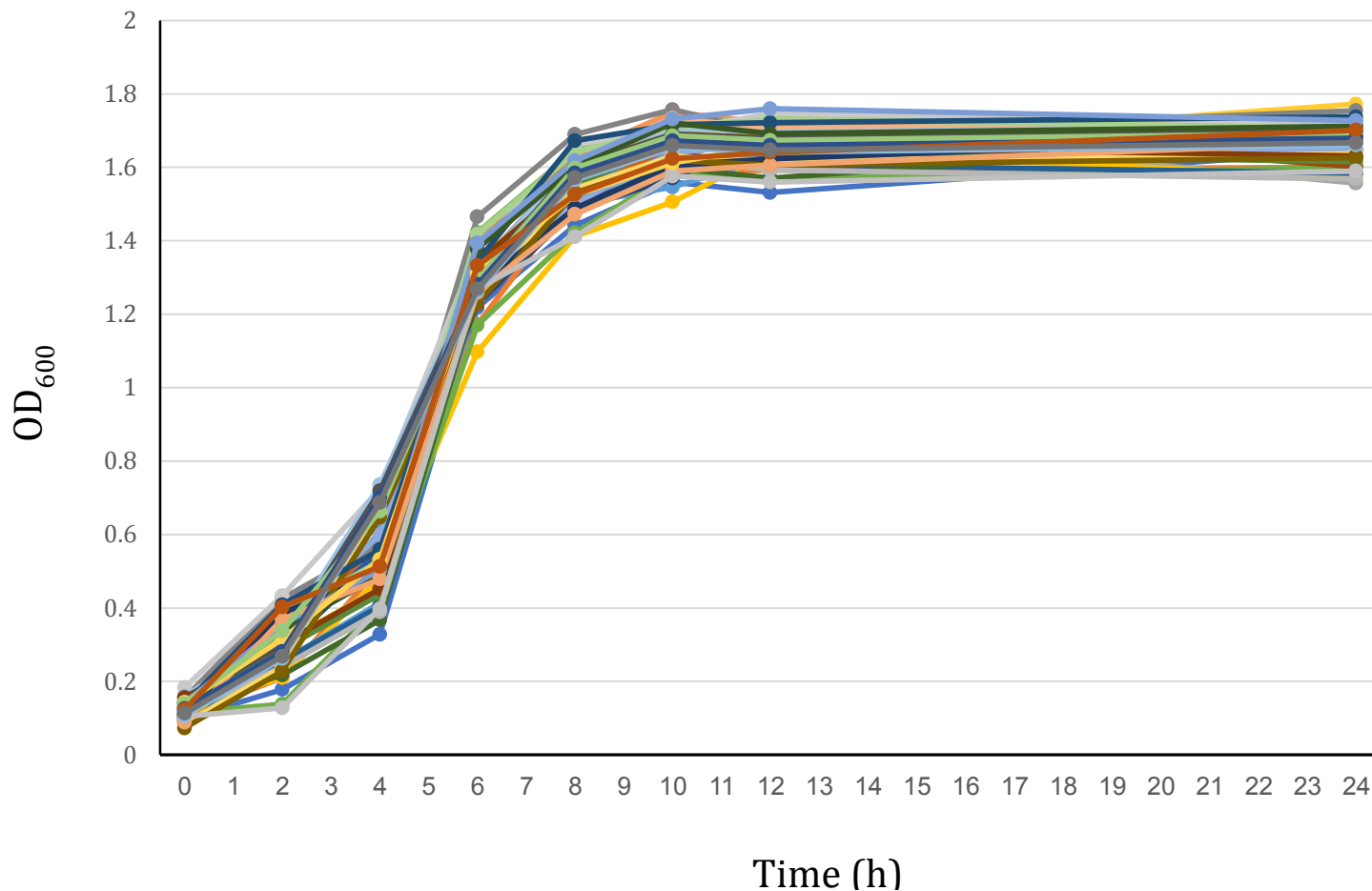


Fig. 5: Growth curves of 46 UPEC isolates of different biofilm formation categories, including strong, moderate, and weak biofilm producers. The X-axis represents the measurement time (h), while the Y-axis represents the measured optical density at 600 nm (OD₆₀₀). The figure shows that no significant differences existed in the growth rates of the tested 46 UPEC isolates, which had different biofilm formation densities. Thus, the differences in biofilm density were not attributed to the differences in the bacterial growth rates.

3.3. Motility assays

The motility assays were performed to determine the swimming and swarming abilities of the UPEC isolates. Wide ranges of motility zones were recorded (Table 1), with swimming zones ranging between 15-53 mm in diameter. The strong biofilm-forming isolates ES5 and ES115 displayed the largest zones of 51 and 53 mm, respectively. The moderate biofilm-forming isolate EM11 produced the smallest swimming zone of 15 mm, followed by the two weak

biofilm-producing isolates EW7 and EW13, both of which had demonstrated a swimming zone diameter of 22 mm. On the other hand, the swarming zones recorded values that ranged between 10-31 mm in diameter. The strong biofilm-producing isolates ES4 and ES5 exhibited the largest swarming zones of 30 and 31 mm, respectively. However, no significant correlation was observed between motility and the biofilm formation capacity ($P > 0.05$). A direct correlation between the swimming and swarming motility ($r_s = 0.506$, $P < 0.001$) was detected (Fig. 6).

Table 1: Summary of the phenotypic virulence characters of the tested forty-six isolates of UPEC

	Swimming zone (mm)	Swarming zone (mm)	Proteolysis zone (mm)	PSU (%) ^b
Range	15 – 53 mm	10 – 31 mm	9 – 39 mm	16.7 - 69.4 %
Highest value (isolate code)	53 mm (ES15) 51 (ES5)	31 mm (ES5) 30 (ES4)	39 mm (EW2) 33 (EW15)	69.4 % (EM13)
Lowest value (isolate code)	15 mm (EM11) 22 (EW7 and EW13)	10 mm (EW7, EM10 and EM11)	9 mm (ES2 and EW3)	16.7 % (EW16)

Where; ^bThe percent siderophore unit (PSU) calculated as follows: $PSU = \frac{(Ar-As)}{Ar} \times 100$

Ar = reference absorbance (CAS-HDTMA solution in sterile broth) and As = sample absorbance (CAS-HDTMA solution in cell-free sample supernatant).

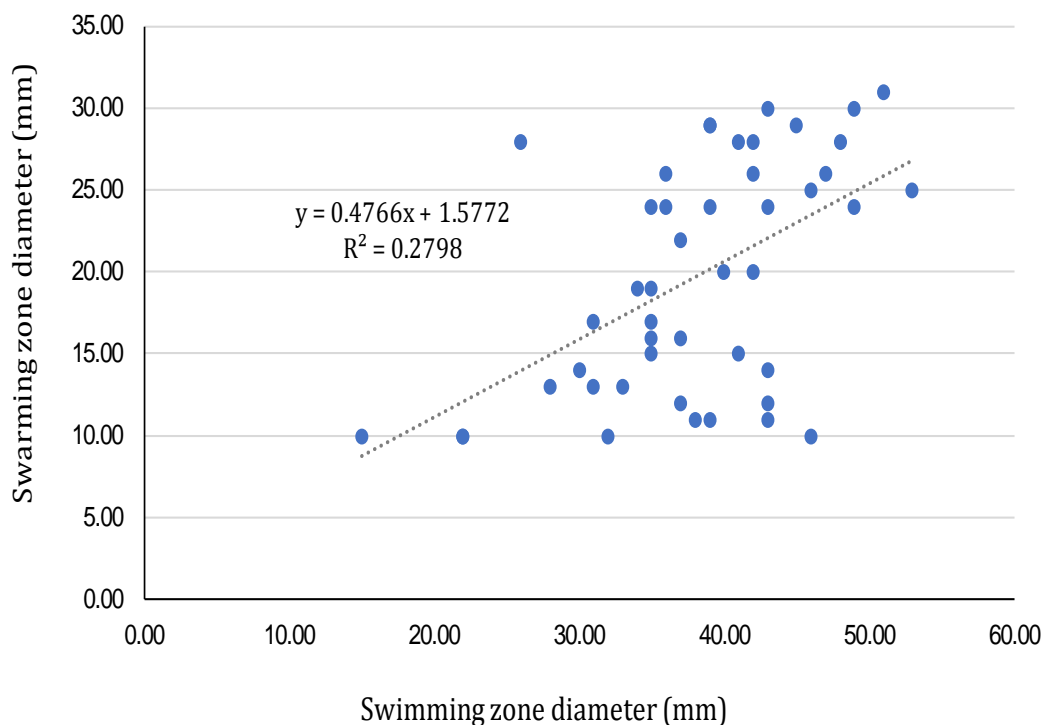


Fig. 6: A scatter plot showing the direct relationship ($P < 0.001$) between the swimming and swarming motilities in the tested UPEC isolates ($n = 46$). The dotted line is the line of best fit that represents the relationship between the two variables. The x value refers to the swimming zone diameter (presented on the X-axis), and the y value refers to the swarming zone diameter (presented on the Y-axis). R^2 is the coefficient of determination.

3.6. Production of protease

Using skim milk agar plates to detect protease production, 40 out of the 46 tested UPEC isolates displayed positive protease production, which was observed as a clear zone of proteolysis around the bacterial growth. Semi-quantitative determination of the protease production was carried out by measuring the diameters of the proteolysis zones. The average lysis zone diameters for the tested isolates ranged between 9-39 mm. The weak biofilm-producing isolates EW2 and EW15 recorded the highest zone diameters of 39 and 33 mm; respectively, whereas the ES2 and EW3 isolates displayed the smallest lysis zones of 9 mm for each (Table 1).

3.5. Siderophore production

The siderophore production levels were measured using the percent siderophore unit (PSU) for each of the tested UPEC isolates ($n = 46$), which revealed that the siderophore production capacity ranged between 16.7-69.4 % compared with 92 % for the EDTA solution (positive control) (Table 1). The siderophore production levels (PSU) were significantly associated with the resistance level to meropenem (measured using the MIC values). The Spearman correlation coefficient for this relationship was $r_s = 0.312$ ($P = 0.035$).

4. Discussion

Uropathogenic *E. coli* (UPEC) is the predominant causative agent of UTIs in both the hospital and community settings (Walker *et al.*, 2022). To our knowledge, up-to-date local information on the effect of biofilm formation on the resistance of clinical UPEC isolates in Tanta, Gharbia governorate, Egypt, is very scarce. Understanding the role of biofilms in antimicrobial resistance and the difference in susceptibility between the planktonic and the biofilm-embedded cells, are essential for accurate treatment of the biofilm-forming bacterial pathogens and for reducing the risk of treatment failure.

Recently, Thöming and Häussler, (2022) reported that bacterial cells in biofilms have up to 1,000-fold higher resistance to antibiotics than the planktonic cells. Biofilm formation reduces the antimicrobial diffusion and can significantly raise a population's effective MIC (Bottery *et al.*, 2021). As a result, bacteria within the biofilm are exposed to sub-inhibitory antimicrobial concentrations that are lower than those outside of the biofilm (Trubenová *et al.*, 2022). When biofilm-forming infections are treated as recommended by the planktonic MIC, the result is that the infection persists and the bacteria recommence their growth after cessation of the antimicrobial agent (Ciofu *et al.*, 2022). Moreover, studies conducted on various bacterial species reported that long-term exposure to sub-inhibitory concentrations of antibiotics promotes biofilm formation, and leads to more enhanced resistance (Thöming and Häussler, 2022; Trubenová *et al.*, 2022).

In the current study, to understand the effect of biofilm development on the sensitivity of the bacterial cells to antimicrobial treatment, the effect of five antimicrobial agents on the planktonic cells and the biofilm-embedded cells was investigated using the MIC and MBEC assays, respectively. Our results revealed that the MIC values were negatively correlated with the biofilm formation category, where strong biofilm producers tended to display lower MIC values for all the tested antibiotics. Several previous studies reported similar observations in *Klebsiella pneumoniae* and *Pseudomonas aeruginosa* (Cusumano *et al.*, 2019; Yamani *et al.*, 2021). These observations may be attributed to fitness costs of the resistance determinants on the bacterial cells, which may affect their virulence and biofilm formation capacity (Cusumano *et al.*, 2019; Trubenová *et al.*, 2022).

Meanwhile, the MBEC values were several folds higher than the MIC values for all the tested antibiotics. These findings reflect the extent of resistance enhancement that biofilms provide to the bacterial cells. The improvement in antibiotic

resistance upon biofilm formation was indicated by the extent of increase (fold difference) in MBEC values compared with the MIC values for each isolate. These fold differences were: 2-256-fold, 8-128-fold, 4-128-fold, 2-128-fold, and 2-64-fold for the cefotaxime, meropenem, ciprofloxacin, amikacin, and cefepime, respectively. The results of the MIC and MBEC analyses agreed with the previous findings of [Amin *et al.*, \(2019\)](#); [Li *et al.*, \(2021\)](#), which demonstrated that biofilm communities have very high levels of antimicrobial resistance compared to their planktonic counterparts, which is indicated by the large differences between the MIC and MBEC values.

Interestingly, there was no significant association between the biofilm resistance (MBEC) and the biofilm formation category ($P > 0.05$). This suggests that the resistance of biofilms to the antibiotics may not only be due to the biofilm density, but also it could be attributed to the presence of persister cells and/ or other genetic factors. This is noteworthy because even bacterial isolates with weak biofilms could still obtain a considerable improvement in their antimicrobial resistance after biofilm formation. On a similar note, [Mah *et al.*, \(2003\)](#) reported that mutations in *P. aeruginosa's ndvB* gene increased the sensitivity of *P. aeruginosa* biofilms to a variety of antibiotics without reducing the *P. aeruginosa* ability to form such biofilms or impairing the biofilm structure. This indicates that the biofilm-specific resistance may depend on factors other than the biofilm density. Similarly, [Qi *et al.*, \(2016\)](#) observed that in *A. baumannii* isolates, the resistance of biofilms (MBEC) was 8-2048 times higher than the resistance of the planktonic cells (MIC) to several antibiotics. This increase in resistance occurred regardless of the amount of the produced biofilm. Moreover, [Shenkutie *et al.*, \(2020\)](#) reported that the biofilm-associated persister cells survived treatment with the antibiotic concentrations that were 256-4096 higher than the MIC values in *A. baumannii* isolates.

UPEC isolates possess a diverse arsenal of virulence factors, which include toxins; serum resistance factors, adhesions, iron acquisition systems,

motility organelles, and others ([Ambite *et al.*, 2021](#)). Flagellar motility is an essential bacterial virulence factor for UPEC, which facilitates ascension of the infection in the urinary tract ([Benyoussef *et al.*, 2022](#)). The swimming and swarming motilities of the tested biofilm-forming UPEC isolates were evaluated, where a strong direct correlation was detected between the two types of flagellar motilities. The detected positive association between the two types of motility may be attributed to the fact that both are powered by flagella ([Wadhwa and Berg, 2022](#)). Although the flagellar motility was speculated to contribute to the various stages in the biofilm formation process in *E. coli*, such as the initial adhesion and the biofilm dispersion ([Khan *et al.*, 2020](#)); however, several studies revealed conflicting results regarding this correlation in the different bacterial species. For instance, many previous studies have reported an inverse correlation between motility and biofilm formation ([O'May *et al.*, 2006](#); [Murray *et al.*, 2010](#)), while others revealed that there is no tangible association between the two factors ([Gajdács *et al.*, 2021a](#); [Behzadi *et al.*, 2022](#)). On the other hand, [Pratt and Kolter, \(1998\)](#) highlighted that the flagella-deficient mutants of *E. coli* had diminished biofilms, due to the essentiality of flagellar motility to the early bacterial attachment and surface spread. Our findings revealed that there was no significant association between motility and biofilm formation capacity and/ or antimicrobial resistance. Proteases are another vital virulence factor of UPEC that have an essential role in facilitating the invasion of the epithelial barriers ([Freire *et al.*, 2022](#)). They also display a wide range of cytotoxic effects and immunomodulatory activities ([Freire *et al.*, 2022](#); [Chen *et al.*, 2023](#)). In the current study, the majority of the tested UPEC isolates produced proteases, and the semi-quantitative analysis demonstrated a large variation in the observed proteolysis zones. A previous recent study conducted by [Reid *et al.*, \(2022\)](#) on the pathogenic *E. coli* strains revealed the carriage of protease genes on large plasmids, such as the *colV* plasmid, which may concurrently carry other virulence and resistance determinants, leading to a positive correlation between protease production and resistance

to the antimicrobials. However, in this study, no association was detected between proteolysis and the biofilm formation capacity, virulence, and/ or antibiotic resistance. In addition, the production of siderophores by UPEC ensures a competitive advantage in acquiring iron in the iron-deficient environment of the urinary tract ([Subashchandrabose and Mobley, 2015](#)). In this study, siderophore production was analyzed using the universal CAS assay, and the resulting siderophore production levels ranged between 16.7-69.4 % PSU. Interestingly, in the current study, siderophore production levels had a significant positive correlation with the meropenem resistance levels (represented by the MIC values). Previous studies conducted by [Karam *et al.*, \(2018\)](#); [El-Baky *et al.*, \(2020\)](#) indicated that certain siderophore genes may be carried on the same mobile genetic elements that also encode for resistance determinants. The combination of resistance and virulence is concerning since it majorly reduces the patients' outcomes and increases the morbidity of the infectious diseases.

Conclusion

Our research highlights the pivotal role of biofilm formation in the context of antibiotic susceptibility of UPEC. The significant disparity between the susceptibility of the bacterial cells in the planktonic and biofilm states emphasizes the essentiality of biofilms for protecting UPEC from the antimicrobial's exposure. Collectively, our findings underscore the importance of taking the biofilm-forming ability into account in the treatment of biofilm-forming UPEC infections, in order to prevent the treatment failure and the infection recurrence. Moreover, the positive correlation between siderophore production and antibiotic resistance; along with the prominence of protease production and bacterial motility in certain isolates, accentuates the complexity of the virulence factors and their distribution in UPEC isolates recovered from Tanta University, Egypt. This study serves as a foundational step towards understanding the effect of biofilm formation on the resistance and virulence levels of UPEC isolates. These findings will

help to pave the way for the development of novel and effective treatment regimens to combat UTIs caused by biofilm-forming UPEC strains.

Acknowledgement

The authors acknowledge the staff members of the Department of Microbiology and Immunology, Tanta University, for their continuous encouragement, and the department's technicians for their aid in the reagents preparation.

Conflict of interest

The authors declare that they have no competing interests.

Funding source

No funding was received to assist with the preparation of this study.

Ethical approval

This study was approved by the Research Ethics Committee of the Faculty of Pharmacy, Tanta University, and assigned an approval code of TP/RE/12/23 p-064.

Authors' Contributions

Conceptualization: T.E., F.S., M.H.F. and S.A.A.; Investigation: S.A.A.; Methodology: S.A.A.; Supervision: T.E., F.S. and M.H.F.; Roles/Writing - original draft: S.A.A.; Writing, reviewing, and editing: T.E., F.S. and M.H.F.

5. References

- Alnahdi, H.S. (2012).** Isolation and screening of extracellular proteases produced by new isolated *Bacillus* sp. *Journal of Applied Pharmaceutical Science*. 2(9): 71-74. <https://doi.org/10.7324/JAPS.2012.2915>
- Ambite, I.; Butler, D.; Wan, M.L.Y.; Rosenblad, T.; Tran, T.H.; Chao, S.M. et al. (2021).** Molecular determinants of disease severity in urinary tract

infection. *Nature Reviews Urology*. 18(8): 468-486.
<https://doi.org/10.1038/s41585-021-00477-x>

Amin, M.; Navidifar, T.; Shoostari, F.S.; Rashno, M.; Savari, M.; Jahangirmehr, F. et al. (2019). Association between biofilm formation, structure, and the expression levels of genes related to biofilm formation and biofilm-specific resistance of *Acinetobacter baumannii* strains isolated from burn infection in Ahvaz, Iran. *Infection and Drug Resistance*. 12: 3867-3881.
<https://doi.org/10.2147/IDR.S228981>

Arora, N.K. and Verma, M. (2017). Modified microplate method for rapid and efficient estimation of siderophore produced by bacteria. *3 Biotech*. 7(6): 381. <https://doi.org/10.1007/s13205-017-1008-y>

Ballén, V.; Cepas, V.; Ratia, C.; Gabasa, Y. and Soto, S.M. (2022a). Clinical *Escherichia coli*: from biofilm formation to new antibiofilm strategies. *Microorganisms*. 10(6): 1103.
<https://doi.org/10.3390/microorganisms10061103>

Ballén, V.; Gabasa, Y.; Ratia, C.; Sánchez, M. and Soto, S. (2022b). Correlation between antimicrobial resistance, virulence determinants and biofilm formation ability among extraintestinal pathogenic *Escherichia coli* strains isolated in Catalonia, Spain. *Frontiers in Microbiology*. 12: 803862.
<https://doi.org/10.3389/fmicb.2021.803862>

Behzadi, P.; Gajdács, M.; Pallós, P.; Ónodi, B.; Stájer, A.; Matusovits, D. et al. (2022) Relationship between biofilm-formation, phenotypic virulence factors and antibiotic resistance in environmental *Pseudomonas aeruginosa*. *Pathogens*. 11(9): 1015.
<https://doi.org/10.3390/pathogens11091015>

Benyoussef, W.; Deforet, M.; Monmeyran, A. and Henry, N. (2022). Flagellar motility during *E. coli* biofilm formation provides a competitive disadvantage which recedes in the presence of co-colonizers. *Frontiers in Cellular and Infection Microbiology*. 12: 896898. <https://doi.org/10.3389/fcimb.2022.896898>

Bottery, M.J.; Pitchford, J.W. and Friman, V.P. (2021). Ecology and evolution of antimicrobial resistance in bacterial communities. *The ISME Journal*. 15(4): 939-948.
<https://doi.org/10.1038/s41396-020-00832-7>

Carcione, D.; Leccese, G.; Conte, G.; Rossi, E.; Intra, J.; Bonomi, A. et al. (2022). Lack of direct correlation between biofilm formation and antimicrobial resistance in clinical *Staphylococcus epidermidis* isolates from an Italian hospital. *Microorganisms*. 10(6): 1163.
<https://doi.org/10.3390/microorganisms10061163>

Chen, Y.C.; Lee, W.C. and Chuang, Y.C. (2023). Emerging non-antibiotic options targeting uropathogenic mechanisms for recurrent uncomplicated urinary tract infection. *International Journal of Molecular Sciences*. 24(8): 7055.
<https://doi.org/10.3390/ijms24087055>

Ciofu, O.; Moser, C.; Jensen, P.Ø. and Høiby, N. (2022). Tolerance and resistance of microbial biofilms. *Nature Reviews Microbiology*. 20(10): 621-635.
<https://doi.org/10.1038/s41579-022-00682-4>

Clinical and Laboratory Standard Institute (CLSI). (2020). Performance Standards for Anti-Microbial Susceptibility Testing. 30th Edition, M100.

Cusumano, J.A.; Caffrey, A.R.; Daffinee, K.E.; Luther, M.K.; Lopes, V. and LaPlante, K.L. (2019). Weak biofilm formation among carbapenem-resistant *Klebsiella pneumoniae*. *Diagnostic Microbiology and Infectious Disease*. 95(4): 114877.
<https://doi.org/10.1016/j.diagmicrobio.2019.114877>

Donadu, M.G.; Ferrari, M.; Mazzarello, V.; Zanetti, S.; Kushkevych, I.; Rittmann, S.K.M.R. et al. (2022). No Correlation between biofilm-forming capacity and antibiotic resistance in environmental *Staphylococcus* spp.: *in vitro* results. *Pathogens*. 11(4): 471. <https://doi.org/10.3390/pathogens11040471>

Eger, E.; Domke, M.; Heiden, S.E.; Paditz, M.; Balau, V.; Huxdorff, C. et al. (2022). Highly virulent

and multidrug-resistant *Escherichia coli* sequence type 58 from a sausage in Germany. *Antibiotics*. 11(8): 1006. <https://doi.org/10.3390/antibiotics11081006>

El-Baky, R.M.A.; Ibrahim, R.A.; Mohamed, D.S.; Ahmed, E.F. and Hashem, Z.S. (2020). Prevalence of virulence genes and their association with antimicrobial resistance among pathogenic *E. coli* isolated from Egyptian patients with different clinical infections. *Infection and Drug Resistance*. 13: 1221–1236. <https://doi.org/10.2147/IDR.S241073>

Freire, C.A.; Silva, R.M.; Ruiz, R.C.; Pimenta, D.C.; Bryant, J.A.; Henderson, I.R. et al. (2022). Secreted autotransporter toxin (Sat) mediates innate immune system evasion. *Frontiers in Immunology*. 13: 844878. <https://doi.org/10.3389/fimmu.2022.844878>

Gajdács, M.; Baráth, Z.; Kárpáti, K.; Szabó, D.; Usai, D.; Zanetti, S. et al. (2021a). No correlation between biofilm formation, virulence factors, and antibiotic resistance in *Pseudomonas aeruginosa*: Results from a laboratory-based *in vitro* study. *Antibiotics*. 10(9): 1134. <https://doi.org/10.3390/antibiotics10091134>

Gajdács, M.; Kárpáti, K.; Nagy, Á.L.; Gugolya, M.; Stájer, A. and Burián, K. (2021b). Association between biofilm-production and antibiotic resistance in *Escherichia coli* isolates: A laboratory-based case study and a literature review. *Acta Microbiologica et Immunologica Hungarica*. 68(4): 217-226. <https://doi.org/10.1556/030.2021.01487>

Hung, K.H.; Wang, M.C.; Huang, A.H.; Yan, J.J. and Wu, J.J. (2012). Heteroresistance to cephalosporins and penicillins in *Acinetobacter baumannii*. *Journal of Clinical Microbiology*. 50(3): 721-626. <https://doi.org/10.1128/JCM.05085-11>

Karam, M.R.A.; Habibi, M. and Bouzari, S. (2018). Relationships between virulence factors and antimicrobial resistance among *Escherichia coli* isolated from urinary tract infections and commensal isolates in Tehran, Iran. *Osong Public Health and*

Research Perspectives. 9(5): 217-224. <https://doi.org/10.24171/j.phrp.2018.9.5.02>

Khan, F.; Tabassum, N.; Pham, D.T.N.; Oloketuyi, S.F. and Kim, Y.M. (2020). Molecules involved in motility regulation in *Escherichia coli* cells: A review. *Biofouling*. 36(8): 889-908. <https://doi.org/10.1080/08927014.2020.1826939>

Li, Z.; Ding, Z.; Liu, Y.; Jin, X.; Xie, J.; Li, T. et al. (2021). Phenotypic and genotypic characteristics of biofilm formation in clinical isolates of *Acinetobacter baumannii*. *Infection and Drug Resistance*. 14: 2613-2624. <https://doi.org/10.2147/IDR.S310081>

Mah, T.F.; Pitts, B.; Pellock, B.; Walker, G.C.; Stewart, P.S. and O'Toole, G.A. (2003). A genetic basis for *Pseudomonas aeruginosa* biofilm antibiotic resistance. *Nature*. 426(6964): 306-310. <https://doi.org/10.1038/nature02122>

Murray, T.S.; Ledizet, M. and Kazmierczak, B.I. (2010). Swarming motility, secretion of type 3 effectors, and biofilm formation phenotypes exhibited within a large cohort of *Pseudomonas aeruginosa* clinical isolates. *Journal of Medical Microbiology*. 59(5): 511-520. <https://doi.org/10.1099/jmm.0.017715-0>

Neilands, B.B. (1987). Universal chemical assay for the detection and determination of siderophores. *Analytical Biochemistry*. 160(1): 47-56. [https://doi.org/10.1016/0003-2697\(87\)90612-9](https://doi.org/10.1016/0003-2697(87)90612-9)

O'May, C.Y.; Reid, D.W. and Kirov, S.M. (2006). Anaerobic culture conditions favor biofilm-like phenotypes in *Pseudomonas aeruginosa* isolates from patients with cystic fibrosis. *FEMS Immunology and Medical Microbiology*. 48(3): 373-380. <https://doi.org/10.1111/j.1574-695X.2006.00157.x>

Pearson, M.M. (2019). Methods for Studying Swarming and Swimming Motility. In: Pearson, M. (Editor) *Proteus mirabilis*. *Methods in Molecular Biology*. Humana, New York. 2021: 15–25. https://doi.org/10.1007/978-1-4939-9601-8_3

- Pratt, L.A. and Kolter, R. (1998).** Genetic analysis of *Escherichia coli* biofilm formation: roles of flagella, motility, chemotaxis and type I pili. *Molecular Microbiology*. 30(2): 285-293. <https://doi.org/10.1046/j.1365-2958.1998.01061.x>
- Qi, L.; Li, H.; Zhang, C.; Liang, B.; Li, J.; Wang, L. et al. (2016).** Relationship between antibiotic resistance, biofilm formation, and biofilm-specific resistance in *Acinetobacter baumannii*. *Frontiers in Microbiology*. 7(4): 483. <https://doi.org/10.3389/fmicb.2016.00483>
- Rafaque, Z.; Abid, N.; Liaqat, N.; Afridi, P.; Siddique, S.; Masood, S. et al. (2020).** *In-vitro* investigation of antibiotics efficacy against uropathogenic *Escherichia coli* biofilms and antibiotic induced biofilm formation at subminimum inhibitory concentration of ciprofloxacin. *Infection and Drug Resistance*. 13: 2801–2810. <https://doi.org/10.2147/IDR.S258355>
- Reid, C.J.; Cummins, M.L.; Börjesson, S.; Brouwer, M.S.; Hasman, H.; Hammerum, A.M. et al. (2022).** A role for *colV* plasmids in the evolution of pathogenic *Escherichia coli* ST58. *Nature Communications*. 13(1): 683. <https://doi.org/10.1038/s41467-022-28342-4>
- Seleem, N.M.; Atallah, H.; Abd El-Latif, H.K.; Shaldam, M.A. and El-Ganiny, A.M. (2021).** Could the analgesic drugs, paracetamol and indomethacin, function as quorum sensing inhibitors? *Microbial Pathogenesis*. 158: 105097. <https://doi.org/10.1016/j.micpath.2021.105097>
- Shenkutie, A.M.; Yao, M.Z.; Siu, G.K.H.; Wong, B.K.C. and Leung, P.H.M. (2020).** Biofilm-induced antibiotic resistance in clinical *Acinetobacter baumannii* isolates. *Antibiotics*. 9(11): 817. <https://doi.org/10.3390/antibiotics9110817>
- Subashchandrabose, S. and Mobley, H.L.T. (2015).** Virulence and fitness determinants of uropathogenic *Escherichia coli*. *Microbiology Spectrum*. 3(4). <https://doi.org/10.1128/microbiolspec.uti-0015-2012>
- Sundaramoorthy, N.S.; Shankaran, P.; Gopalan, V. and Nagarajan, S. (2022).** New tools to mitigate drug resistance in *Enterobacteriaceae–Escherichia coli* and *Klebsiella pneumoniae*. *Critical Reviews in Microbiology*. 49(4): 435-454. <https://doi.org/10.1080/1040841X.2022.2080525>
- Terlizzi, M.E.; Gribaudo, G. and Maffei, M.E. (2017).** Uropathogenic *Escherichia coli* (UPEC) infections: Virulence factors, bladder responses, antibiotic, and non-antibiotic antimicrobial strategies. *Frontiers in Microbiology*. 8: 1566. <https://doi.org/10.3389/fmicb.2017.01566>
- Thöming, J.G. and Häussler, S. (2022).** *Pseudomonas aeruginosa* is more tolerant under biofilm than under planktonic growth conditions: a multi-isolate survey. *Frontiers in Cellular and Infection Microbiology*. 12: 851784. <https://doi.org/10.3389/fcimb.2022.851784>
- Torres-Puig, S.; García, V.; Stærk, K.; Andersen, T.E.; Møller-Jensen, J.; Olsen, J.E. et al. (2022).** “Omics” technologies - what have they told us about uropathogenic *Escherichia coli* fitness and virulence during urinary tract infection? *Frontiers in Cellular and Infection Microbiology*. 12: 824039. <https://doi.org/10.3389/fcimb.2022.824039>
- Trubenová, B.; Roizman, D.; Moter, A.; Rolff, J. and Regoes, R.R. (2022).** Population genetics, biofilm recalcitrance, and antibiotic resistance evolution. *Trends in Microbiology*. 30(9): 841-852. <https://doi.org/10.1016/j.tim.2022.02.005>
- Vega-Hernández, R.; Ochoa, S.A.; Valle-Rios, R.; Jaimes-Ortega, G.A.; Arellano-Galindo, J.; Aparicio-Ozores, G. et al. (2021).** Flagella, type I fimbriae and curli of uropathogenic *Escherichia coli* promote the release of proinflammatory cytokines in a coculture system. *Microorganisms*. 9(11): 2233. <https://doi.org/10.3390/microorganisms9112233>
- Wadhwa, N. and Berg, H.C. (2022).** Bacterial motility: machinery and mechanisms. *Nature Reviews*

Microbiology. 20(3): 161-173.
<https://doi.org/10.1038/s41579-021-00626-4>

Walker, M.M.; Roberts, J.A.; Rogers, B.A.; Harris, P.N.A. and Sime, F.B. (2022). Current and emerging treatment options for multidrug-resistant *Escherichia coli* urosepsis: A review. *Antibiotics*. 11(12): 1821.
<https://doi.org/10.3390/antibiotics11121821>

Whelan, S.; Lucey, B. and Finn, K. (2023). Uropathogenic *Escherichia coli* (UPEC)-associated urinary tract infections: the molecular basis for challenges to effective treatment. *Microorganisms*. 11(9): 2169.
<https://doi.org/10.3390/microorganisms11092169>

Yamani, L.; Alamri, A.; Alsultan, A.; Alfifi, S.; Ansari, M.A. and Alnimr, A. (2021). Inverse correlation between biofilm production efficiency and antimicrobial resistance in clinical isolates of *Pseudomonas aeruginosa*. *Microbial Pathogenesis*. 157: 104989.
<https://doi.org/10.1016/j.micpath.2021.104989>